

Numerical study of neoclassical particle losses with static 2D electric fields

A. Salmi¹, V. Parail², T. Johnson³, C. S. Chang⁴, S. Ku⁴, G. Park⁴ and JET EFDA contributors*

JET-EFDA, Culham Science Center, OX14 3DB, Abingdon, UK

¹*Association EURATOM-Tekes, TKK, Advanced Energy Systems, PO Box 4100, 02015 HUT, Finland*

²*Culham Science Centre, EURATOM/UKAEA Association, OX14 3DB, Abingdon, UK*

³*Association EURATOM - VR, Fusion Plasma Physics, EES, KTH, Stockholm, Sweden*

⁴*Courant Institute of Mathematical Sciences, New York University, New York, USA*

**See the Appendix of M.L. Watkins et al., Fusion Energy 2006 (Proc. 21st Int. Conf. Chengdu) IAEA, (2006)*

Reduced particle confinement (often referred to as “density pump-out”) has been observed in magnetically confined fusion plasma experiments where non-ambipolar particle losses are expected, e.g. in ripple and resonant magnetic field (RMP) experiments [1]. It has been proposed that the so-called “convective cells” or poloidally localised 2D electric fields could be at least partly responsible for the confinement degradation [2].

In this contribution we study the neoclassical particle losses in the presence of an axisymmetric, electrostatic, 2D potential. As a simulation tool for this analysis we use XGC-0 which is a guiding centre following Monte Carlo code developed for resolving neoclassical transport[3]. XGC-0 is able to follow both ions and electrons and it solves the radial electric field self-consistently from the radial current balance[4]. On top of the existing functionality a model for a static axisymmetric 2D gaussian potential was added. We use this set-up to estimate how large the 2D perturbation has to be to have a non-negligible effect. If found to be relatively modest then more CPU time consuming 2D/3D Poisson equation solving self-consistent codes could be used together with the loss mechanisms to see whether such poloidal potential variations can exist.

In the simulations we use EFIT reconstruction of JET discharge #60856 for magnetic background. We limit the simulation region to the edge of the plasma covering a range $\Psi_n=[0.85,1.03]$ in normalised poloidal flux co-ordinate. We initialise the test particles, electrons and deuterons, to follow hyperbolic tangent profiles with a pedestal width $\Delta\Psi_n^{ped} = 0.03$, pedestal top temperature $T_{ped} = 1.0\text{keV}$ and density $n_{ped} = 2 \cdot 10^{19} m^{-3}$ as shown in Figure 1. Also shown are the locations (X-point & midplane) used for the 2D gaussian potentials and an example of the self-consistent radial potential predicted by the simulations.

The half width of the gaussian potentials has been fixed to 17cm for all simulations and the unperturbed banana width of a thermal ion at the top of the pedestal is roughly $\Delta\Psi_n^{banana} \approx 0.02$. Fixed maxwellian background collision model is used.

Figure 2 illustrates the characteristic effect that the introduction of the 2D potential well has on collisionless particle orbits. In an axi-symmetric situation, like here, the particles conserve both the canonical toroidal momentum

$$p_\phi = Ze\Psi + Rm v_\phi$$

and the magnetic moment $\mu = E_\perp/B$. The conservation of the magnetic

moment means that the extra kinetic energy gained, when falling in the potential, increases only the parallel velocity of the particle. From the above equations one can also see that the deviation, $\Delta\Psi$, of the guiding centre from the flux surface is essentially proportional to $\Delta v_\phi \approx \Delta v_\parallel \cdot B_\phi/B$. Thus; an attractive (repulsive) potential will move the particle further away from (closer to) the bounce averaged flux surface. The main difference between the X-point and the midplane perturbations is that only the X-point perturbation can transform an initially confined orbit into a loss orbit without collisions as shown in the subplot on lower right.

The conservation of the magnetic moment means that the extra kinetic energy gained, when falling in the potential, increases only the parallel velocity of the particle. From the above equations one can also see that the deviation, $\Delta\Psi$, of the guiding centre from the flux surface is essentially proportional to $\Delta v_\phi \approx \Delta v_\parallel \cdot B_\phi/B$. Thus; an attractive (repulsive) potential will move the particle further away from (closer to) the bounce averaged flux surface. The main difference between the X-point and the midplane perturbations is that only the X-point perturbation can transform an initially confined orbit into a loss orbit without collisions as shown in the subplot on lower right.

In full simulations including collisions and the self-consistent radial electric field we start the simulation without the perturbation to allow the system to relax and to establish the 1D self-consistent radial electric field before turning on the perturbation. Figure 3 shows the instantaneous particle content inside separatrix for two cases; one without the static 2D

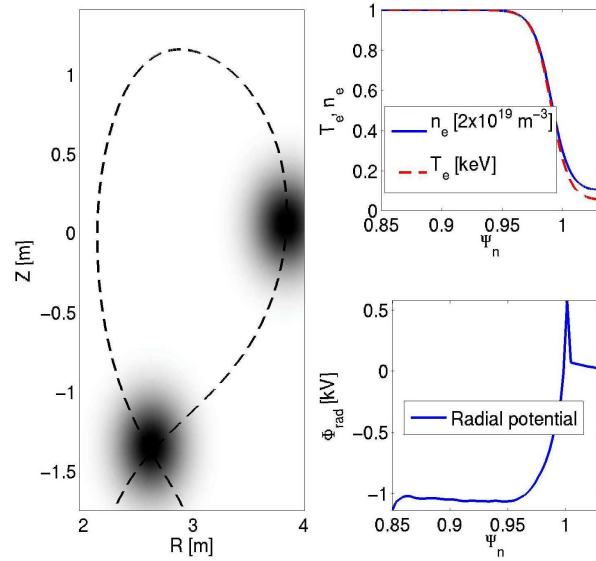


Figure 1 a) Locations used for the 2D gaussian potentials, b) initial density and temperature profiles (Ti=Te, Ni=Ne) and c) typical self-consistent radial potential. Radial co-ordinate is the normalised poloidal

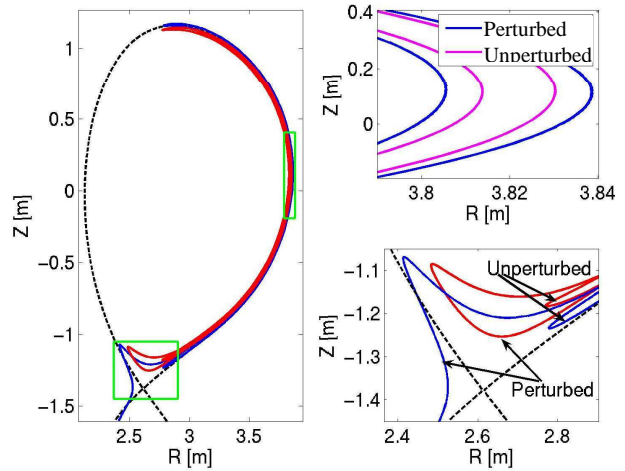


Figure 2 Illustrations of the effect of a 2D electrostatic perturbation ($\Phi_{min}=-500V$) on 1 keV deuteron orbits. Perturbations were placed both on X-point and on midplane. Green squares indicate the zoom-in region for the figures on the right.

perturbation and the other where the perturbation is half of the pedestal top temperature ($Ze\Phi_{\min} = -kT_{\text{ped}}/2$). For both cases the average flux of particles, even before the 2D potential onset, is directed outwards since we do not include particle sources to keep the analysis as unambiguous as possible. The depletion rate of the particle content remains, however, relatively constant after the initial transition at the start of the simulation and after the onset of the perturbation. To estimate the effect of the 2D perturbation more quantitatively we compare the perturbed loss rates against the unperturbed reference case. Loss rates are averaged over the last part of the simulation as indicated by the shadowed region on the right of Figure 3.

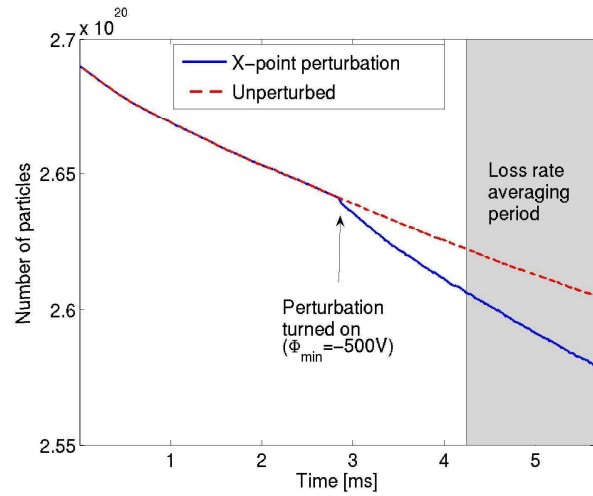


Figure 3 Particle inventory inside separatrix.

Figure 4 shows the main result: the enhancement of the particle flux through the separatrix by the application of the 2D potential. The scan performed shows that the stronger the perturbation the higher the loss rate becomes. It also shows that a potential of the order of 1/5 or even 1/10 of the pedestal top temperature could be sufficient to enhance the neoclassical losses by about 10-30%. We see that as could be expected the X-point perturbation is more effective in enhancing the losses for the lower end of the perturbation strength. The saturation in the effectiveness of the X-point perturbation beyond -250V results from the increased capability of the 2D potential to reflect electrons and effectively prevent a large population of them to reach the divertor. Consequently, radial outward electron current is reduced and the self-consistent radial electric field becomes such that it leads to an improved ion confinement (via orbit squeezing). When the perturbation is at midplane electron losses are not clamped and losses increase with the perturbation strength.

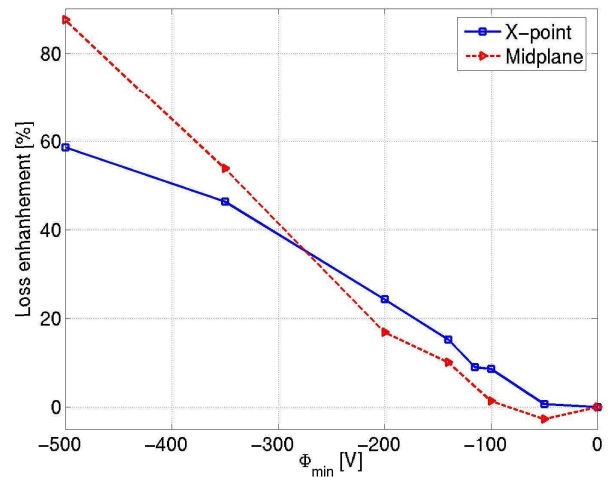


Figure 4 Loss rate enhancement with 2D perturbation.

When analysing collisionless orbits one might conclude that only X-point perturbation could enhance the loss rate since the perturbed orbit away from the X-point will quickly assume the same flux surface it had prior the perturbation. However, even a local attractive perturbation increases the time a particle spends away from its average flux surface, $\bar{\Psi}$, and thus leads to an enhanced collisional diffusion $D \sim (\Delta\Psi)^2/\tau_c$. Figure 5 shows the average displacement of a deuteron $\langle \Delta\Psi_n \rangle = \oint dt |\bar{\Psi}_n - \Psi_n(t)| / \oint dt$ with 1keV Hamiltonian energy as a function of pitch measured at midplane. Here, as already seen

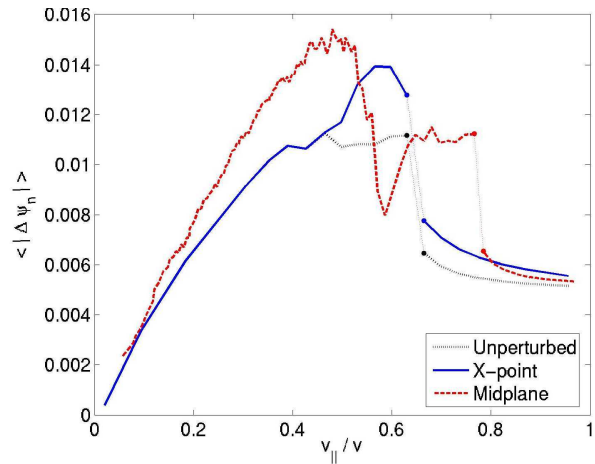


Figure 5 Average orbit width of a 1keV deuteron w/ and w/o -500V perturbations.

in Figure 2, particles close to passing-trapped boundary (these have their turning points in the vicinity of the X-point perturbation) are mostly influenced by the X-point perturbation. On the other hand, the midplane perturbation is very effective in maintaining the orbit width of trapped particles thus greatly enhancing the diffusion in this part of the phase space. The result as seen in full simulations is the enhancement of neoclassical losses for both cases. For the midplane perturbation it is solely the enhanced collisional diffusion that gives the extra losses.

Our simulations with XGC-0 would, in principle, indicate that a 2D potential is a viable candidate for contributing to the density pump-out. To evaluate the amplitude of the potential perturbation and thus the losses that are sustainable one would, however, have to solve the Poisson equation self-consistently in 2D including the loss mechanisms.

Acknowledgement: This work, supported by the European Communities under the contract of Association between EURATOM/TEKES, was carried out within the framework of the European Fusion Development Agreement. The views and opinions expressed herein do not necessarily reflect those of the European Commission.

- [1] V. Parail et al., Proceedings of the 21st IAEA Conference, Chengdu, TH/P8-5, (2006)
- [2] T. E. Evans et al., Nuclear Fusion, 45 595 (2005)
- [3] C. S. Chang, S. Ku and H. Weizener, Phys. Plasmas 11 2649 (2004)
- [4] J. A. Heikkinen, T. P. Kiviniemi, and A. G. Peeters, Phys. Rev. Lett., 84 487 (2000)